Research on wavelength conversion of triangular pulses with variable symmetry based on SPM effect*

YUAN Jin, LIU Qisong, MEI Ying, XU Xiuxiu, WANG Yujie, and BA Xinran**

State Key Laboratory of Media Convergence and Communication, Communication University of China, Beijing 100044, China

(Received 29 June 2022; Revised 9 March 2023)

The generation of periodic triangular waveform with variable symmetrical coefficient based on a dual-parallel Mach-Zehnder modulator (DP-MZM) is demonstrated in this work. By properly setting the modulation index and bias points of DP-MZM, desired symmetric/asymmetric triangular waveforms can be generated. Then applying the generated triangular waveform into an amplitude modulator (AM), a single-period signal can be extracted to explore the optical wavelength conversion induced by the self-phase modulation (SPM) effect in a high nonlinear fiber (HNLF). Wavelength shifts of triangular waveforms with different coefficients (10%, 20%, 30%, 40% and 50%) are calculated. In addition, the influence of key parameters of HNLF on the wavelength conversion is analyzed in detail.

Document code: A **Article ID:** 1673-1905(2023)08-0449-6

DOI https://doi.org/10.1007/s11801-023-2116-z

The current communication network is in a stage of rapid development with continuous demands for capacity and increasingly tight frequency resources. The radio over fiber (ROF) utilizes optical fiber as the signal transmitter, which improves the capacity dramatically[1-4]. Microwave arbitrary waveforms are widely used in radar, communications, medical imaging, and modern instrumentation systems[5,6]. Optical triangular waveform featured with linear rising-edge and falling-edge in intensity can be used for various applications, such as optical signal access, wavelength conversion and optical pulse compression, which are indispensable for future all-optical networks[7,8]. Thus the researches about generation of triangular waveform are more indispensable.

Recently, various approaches for the generation of triangular waveforms have been proposed[9-16]. The proposal based on the frequency-to-time mapping (FTTM) technique could be used in arbitrary optical pulse generator[10]. Ref.[11] put forwards a new method to generate microwave waveform by phase modulation and optical carrier phase processing based on gain-transparent stimulated Brillouin scattering (SBS). However, the inadequacies of such schemes are the high cost and low flexibility. Thus, approaches based on external modulation, including Mach-Zehnder modulators (MZMs), phase modulator (PM) and polarization modulator[12-20], are proposed. In Ref.[14], a photonic microwave waveform generator utilizing a dual-drive Mach-Zehnder modulator (DD-MZM) is proposed and experimentally demonstrated. Optoelectronic oscillators (OEOs) are also widely used in waveform photonic generation. In Ref.[15], a dual-parallel Mach-Zehnder modulator (DP-MZM), with the assistance of OEO which provides continuous oscillation at two orthogonal polarizations frequencies, is employed to obtain triangular waveform. Generation of triangular waveform with variable symmetry is presented, which provides more potential advantages on the applications of the triangular-shaped pulses. In Ref.[21], a DP-MZM is used to generate an optical triangular waveform with variable symmetry. In Ref.[22], an approach for triangular waveform generation with an adjustable symmetrical coefficient is proposed based on a single SD-MZM. In Ref.[23], the authors utilize a DP-MZM and a balanced photodetector to realize the generation of signals with a quadruple frequency and a triangular waveform tunable in symmetry.

All-optical waveform conversion is likely to represent a key function within future optical communication systems since it can be used to avoid wavelength blocking and give flexibility in network design[24,25]. In Refs.[24] and [25], a saw-tooth input signal pulse shape (asymmetric triangular) is the key to improve the efficiency of the wavelength conversion system is proved. The wavelength conversion system is based on self-phase modulation (SPM) or cross-phase modulation (XPM).

In this paper, we propose a periodic triangular waveform generator with variable symmetry based on a DP-MZM and investigate its application in optical wavelength conversion. Optical carrier suppression (OCS) modulation is conducted in a DP-MZM to obtain

* This work has been supported by the National Natural Science Foundation of China (No.62105306), and the Fundamental Natural Funds for the Central Universities (No.CUC230B021).

** E-mail: baxinran@cuc.edu.cn

the desired optical spectra corresponding to target triangular waveforms. The feasibility has been proved in our previous work[26]. To analyze the wavelength conversion more intuitively, we extract a single triangular pulse from the generated pulse train. This work mainly presents the principles of variable symmetry triangular waveform generation and its wavelength conversion caused by the SPM effect in a high nonlinear fiber (HNLF). This work gives a comprehensive analysis and discussion of the generation and application of triangular pulses with variable symmetry.

The proposed variable symmetry triangular waveform generator is shown in Fig.1. The continuous optical signal emitted by continuous wave (CW) light source is defined as $E_{\rm in}(t)=E_0\cos(\omega_0 t)$, where E_0 and ω_0 represent the amplitude and frequency, respectively. The DP-MZM consists of two sub-MZMs (MZ-a and MZ-b) and a parent-MZM (MZ-c), of which the bias voltage is $V_{\rm bias1}$, $V_{\rm bias2}$ and $V_{\rm bias3}$, respectively. A phase shifter (PS) is applied to introduce a phase shift Φ between RF driving signals of MZ-a and MZ-b, which are defined as $V_{\rm LO}\cdot\cos(\Omega_m t)$ and $V_{\rm LO}\cos(\Omega_m t+\Phi)$, where $V_{\rm LO}$ and $\Omega=2\pi f$ are the amplitude and frequency.

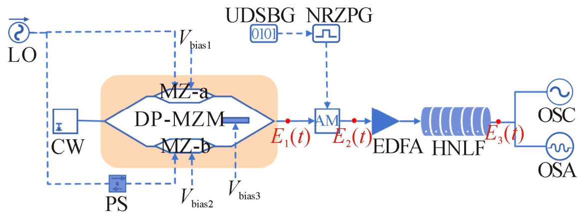

Fig.1 Schematic diagram of the proposed variable symmetry triangular waveform generator

The optical field of the signal at DP-MZM output can be expressed as

$$E_1(t)=E_{\rm in}(t)\{\cos[m\cos(\Omega t)-\frac{\varphi_1}{2}]\exp(\mathrm{j}\frac{\varphi_1}{2})+\cos[m\cos(\Omega t-\Phi)-\frac{\varphi_2}{2}]\exp(\mathrm{j}\frac{\varphi_2}{2}+\mathrm{j}\varphi_3)\},\quad(1)$$

where $m=\pi V_{\rm LO}/2V_\pi$ denotes the modulation index of the DP-MZM and $\varphi_{1,2,3}=\pi V_{\rm bias1,2,3}/V_\pi$ is the phase shift introduced by the bias voltage, where V_π is the half-wave switching voltage. Carrying out Jacobi-Anger expansion, when $\varphi_2-\varphi_1=\pi$ and $\varphi_3=k\pi$, $k\in\mathrm{N}^+$, the corresponding photocurrent of $E_1(t)$ can be written as

$$I_1(t)=E_0^2+\sum_{n=1}^{\infty}\{\alpha_{2n-1}\sin[(2n-1)(\Omega t-\Phi/2)]+\alpha_{2n}\sin[2n(\Omega t-\Phi/2)]\},\quad(2)$$

where

$$\alpha_{2n-1}=2(-1)^n E_0^2\sin\varphi_1\cdot J_{2n-1}(2m)\cdot\sin[(2n-1)\Phi/2],\quad(3)$$

$$\alpha_{2n}=2(-1)^{n+1}E_0^2\cos\varphi_1\cdot J_{2n}(2m)\cdot\sin[2n\cdot\Phi/2],\quad(4)$$

where $J(\cdot)$ represents the Bessel function of the first kind.

The expansion of triangular waveform with a symmetrical coefficient of δ can be expressed as

$$S(t)=\sum_{n=1}^{\infty}\beta_n\sin(n\omega t),$$

$$\beta_n=\frac{\omega}{\pi}\int_{-\frac{\delta T}{2}}^{T-\frac{\delta T}{2}}S_{\rm single}(t)\sin(n\omega t)\mathrm{d}t.\quad(5)$$

As triangular waveform is generated by harmonic fitting of the first two components[15], $I_1(t)$ can be simplified as

$$I_1\approx\alpha_1\sin(\Omega t-\frac{\Phi}{2})+\alpha_2\sin[2(\Omega t-\frac{\Phi}{2})]+\alpha_3\sin[3(\Omega t-\frac{\Phi}{2})].\quad(6)$$

Comparing Eq.(5) and Eq.(6), following equation should be satisfied.

$$\alpha_1:\alpha_2:\alpha_3=\beta_1:\beta_2:\beta_3.\quad(7)$$

Substituting Eqs.(3—6) into Eq.(7), it can be calculated as

$$\Phi=\arccos[-\frac{\beta_3 J_1(2m)+\beta_1 J_3(2m)}{2\beta_1 J_3(2m)}],\quad(8)$$

$$\varphi_1=\arctan\sqrt{\frac{\beta_1^2 J_2^2(2m)J_3(2m)-\beta_1\beta_3 J_1(2m)J_2^2(2m)}{\beta_2^2 J_1^2(2m)J_3(2m)}}.\quad(9)$$

From the above analysis, by properly setting the values of Φ and φ_1 and m, triangular waveform with desired symmetrical coefficient δ can be obtained.

As in Fig.1, when the obtained triangular waveform signal transmitted in the HNLF, the SPM effect may induce new frequency components generation. Thus, the energy has been transferred to the new frequencies efficiently and achieved the wavelength conversion in optical spectrum. We firstly extract a triangular pulse with a single period by using an AM driven by an electrical signal form an NRZPG as in Fig.1. Then the single triangular pulse is amplified by an erbium-doped fiber amplifier (EDFA) and enters an HNLF for SPM effect.

Frequency shift $\sigma\omega(t)$ is defined to evaluate the spectral broadening, and its mathematical calculation can be described as[27]

$$\sigma\omega(t)=-\frac{\partial\phi_{\rm nl}}{\partial t}=-L\gamma P_0\frac{\partial|u(0,t)|^2}{\partial t},\quad(10)$$

where L is the length, $\gamma=\omega_0 n_2/cA_{\rm eff}$ is the nonlinear coefficient and $A_{\rm eff}$ is the mode area of HNLF. P_0 and $u(0,t)$ represent the peak average power and normalized envelope of the generated triangular waveform. Form Eq.(10), it can be seen that for a certain input optical pulse, the frequency shift is related to L, $A_{\rm eff}$, P_0, and the rate of change of optical intensity over time. Triangular waveform with different symmetrical coefficient δ has different expression of $u(0,t)$.

The proposed variable symmetry triangular waveform generation is simulated in Optisystem. The CW optical signal has a center wavelength of 1 550 nm, an optical power of 10 dBm, and a linewidth of 0.8 MHz. The RF driving signal is 10 GHz and the modulation index is

m=1.1. The detailed parameter setting is as shown in Tab.1.

Tab.1 Parameter setting

δ (%)	φ (rad)	Φ (rad)	V_{bias1} (V)	V_{bias2} (V)
10	0.71	2.615	4.89	0.89
20	0.979 2	2.396	5.25	1.25
30	1.2	2.18	5.53	1.53
40	1.4	1.98	5.78	1.78
50	1.57	1.89	6.01	2.01

The simulation results of the output signal after the DP-MZM are shown in Fig.2. It can be seen that the full-duty-cycle triangular waveforms with adjustable symmetrical coefficient δ (10%, 20%, 30%, 40% and 50%) are acquired. Comparing with Ref.[23], the desired modulation index in this scheme is smaller.

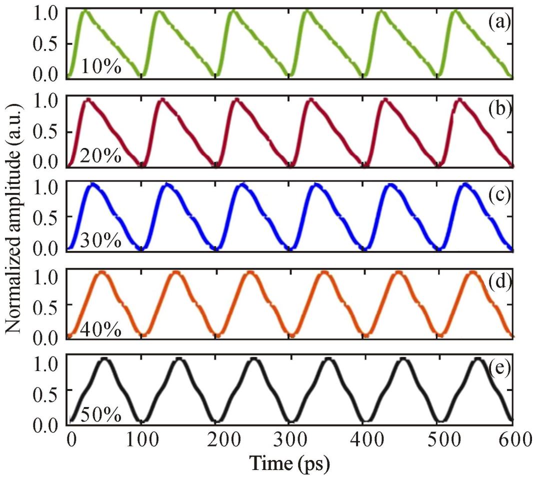

Fig.2 Temporal triangular waveforms with (a) δ=10%, (b) δ=20%, (c) δ=30%, (d) δ=40%, and (e) δ=50%

To analyze the wavelength conversion of symmetrical triangular waveform intuitively, we extract a one-period pulse signal from the pulse train by using an AM for secondary modulation. Fig.3(a) is temporal waveform and optical spectrum of the one-period symmetrical triangular waveform, of which the full-width is 100 ps and the slopes of the rising and falling edges are linear and symmetric. The corresponding optical spectrum of the extracted signal is with a center wavelength of 1 550 nm, and no new frequency component is generated.

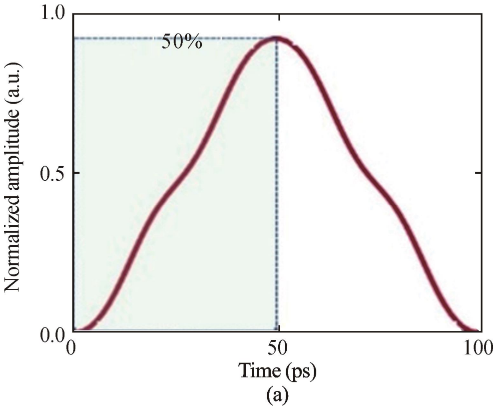

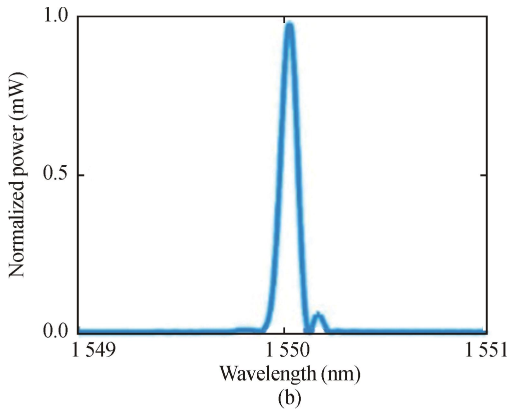

Fig.3 (a) Temporal waveform and (b) optical spectrum of the one-period symmetrical triangular waveform

Then the one-period triangular waveform is amplified by an EDFA and enters the HNLF, in which wavelength conversion can be induced due to the SPM effect. To analyze the wavelength conversion, we introduce a concept of wavelength shift ($\Delta\lambda$), which represents the center wavelength difference between triangular waveform before and after HNLF. It can be seen that fiber length L and effective mode area A_{eff} of the HNLF may influence the value of $\Delta\lambda$. Results in Fig.4 show the relation between $\Delta\lambda$ and A_{eff}, when L is set as 0.1 km. It can be seen that due to the SMP effect, the center wavelength of triangular waveform shifts symmetrically to both sides. With the increase of A_{eff}, the value of $\Delta\lambda$ turns out to be declined, which agrees well with Eq.(10). Specifically, when A_{eff} is 2 μm^2, 4 μm^2, and 5 μm^2, the corresponding $\Delta\lambda$ is 0.594 3 nm, 0.238 8 nm and 0.181 3 nm.

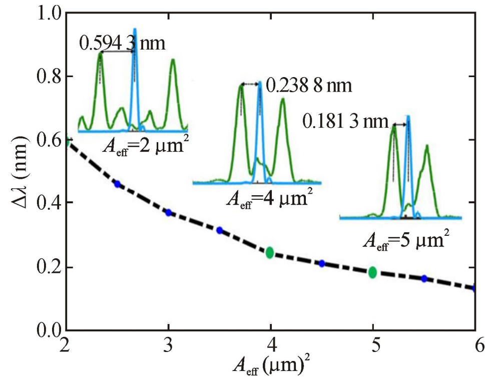

Fig.4 Relationship between A_{eff} and $\Delta\lambda$ for the one-period symmetrical triangular waveform

Fig.5 illustrates the relationship between L and $\Delta\lambda$ when A_{eff} is set as A_{eff}=2 μm^2. When the value of L increases from 0.05 km to 0.1 km, $\Delta\lambda$ also increases. Specifically, when L is 0.05 km, 0.08 km, and 0.1 km, the corresponding $\Delta\lambda$ is 0.263 2 nm, 0.472 3 nm and 0.594 3 nm.

To analyze the wavelength conversion of asymmetrical triangular waveform, we taking a triangular waveform with symmetry coefficient δ=20% as an example for analysis. A one-period triangular waveform is also extracted, of which the temporal and optical spectra are as shown in Fig.6.

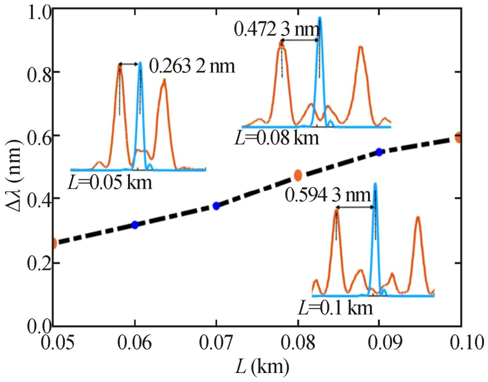

Fig.5 Relationship between *L* and Δ*λ* for the one-period symmetrical triangular waveform

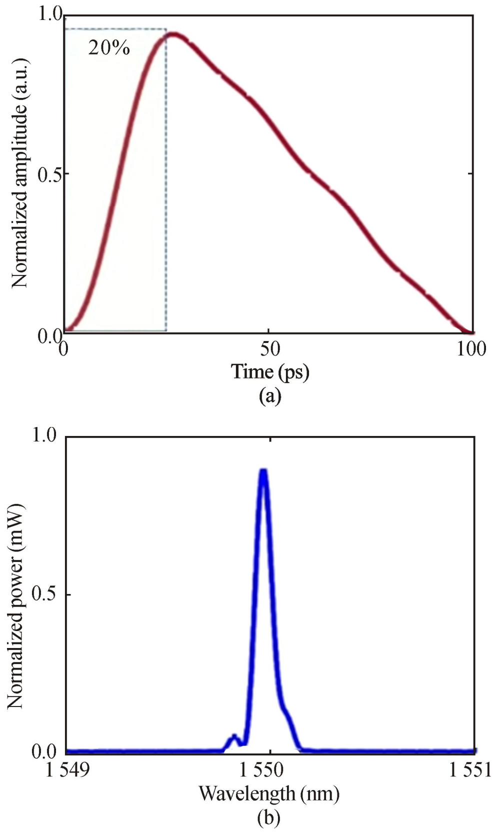

Fig.6 (a) Temporal waveform and (b) optical spectrum of the triangular waveform with *δ*=20%

We also analyze the wavelength conversion of the triangular waveform with δ=20%. Results in Fig.7 and Fig.8 give the wavelength conversion for different parameters of HNLF. From the illustrations we can see that after SPM effect in HNLF, the center wavelength of triangular waveform shift to one side, and the value of $\Delta\lambda$ is related to parameters of HNLF according to Eq.(10). As in Fig.7, when L is set as 0.1 km, $\Delta\lambda$ declines with the increasement of A_{eff}. Specifically, when A_{eff} is 1.5 μm^2, 3 μm^2, and 4.5 μm^2, $\Delta\lambda$ is 0.636 8 nm, 0.336 5 nm and 0.237 6 nm. In Fig.8, when A_{eff} is set as 2 μm^2, $\Delta\lambda$ increases with the increasement of L. When L is 0.12 km, 0.16 km, and 0.18 km, $\Delta\lambda$ is 0.763 2 nm, 1.010 8 nm and 1.238 4 nm. These results are aligned with Eq.(10).

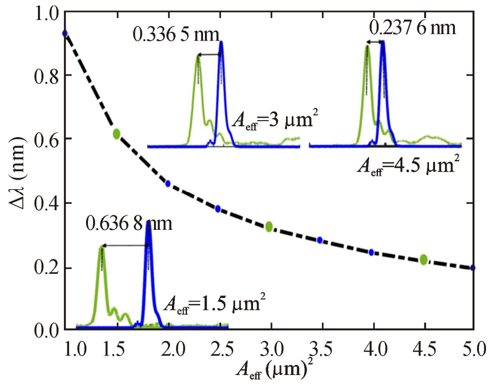

Fig.7 Relationship between A_{eff} and Δ*λ* for the triangular waveform with *δ*=20%

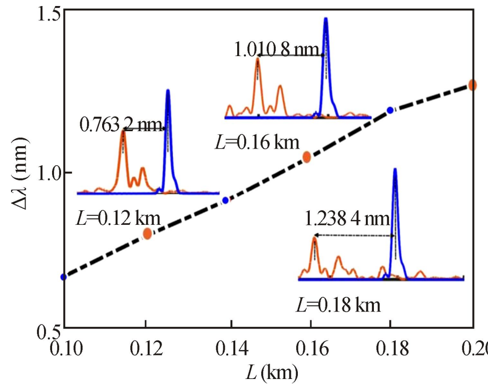

Fig.8 Relationship between *L* and Δ*λ* for the triangular waveform with *δ*=20%

To further analyze the wavelength conversion of triangular waveforms, we simulate the wavelength conversion of triangular waveforms with different symmetry coefficients δ (10%, 20%, 30%, 40% and 50%) as in Fig.9(a). Taking HNLF with A_{eff}=2 μm^2 and L=0.1 km for example, it can be seen from the spectrum evolution that after SPM effect, the wavelength of triangular waveform shifts to two new frequencies. Differently, the optical spectrum of triangular waveform with δ of 50% is symmetrical after evolution, while the triangular waveforms with δ of 10%, 20%, 30% and 40% are asymmetrical. Fig.9(b) reveals the wavelength shift $\Delta\lambda$ versus different δ, from which we can see that for a larger δ, the wavelength shift is more obvious. However, results in Fig.9(a) prove that when the spectrum on one side is filtered out and used, there will exist more power loss for a triangular waveform with larger δ. That is to say, there is a trade-off between the power and the wavelength shift after wavelength conversion.

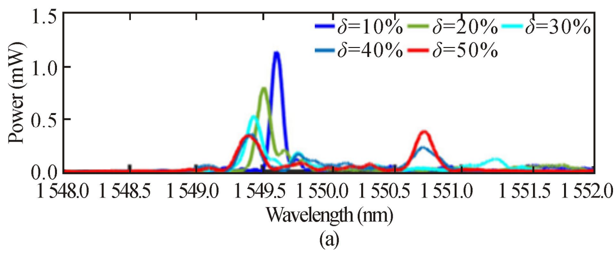

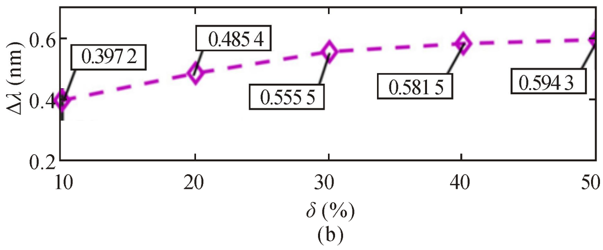

Fig.9 (a) Optical spectra of the triangular waveform with different *δ*; (b) Relationship between Δ*λ* and *δ*

This work proposed a photonic approach to generate triangular waveform with variable symmetry coefficients based on harmonic fitting. As a 5-GHz RF driving signal is applied, a full-duty-cycle triangular waveform with adjustable symmetrical coefficient δ of 10%, 20%, 30%, 40% and 50% is generated. In addition, we analyze the wavelength conversion, which is induced by the SPM effect in an HNLF, of triangular waveforms with different δ. Particularly, we calculate the wavelength conversion of triangular waveform with δ of 50% and 20% and analyze the influence of parameters of HNLF (L and A_{eff}) on wavelength shift ($\Delta\lambda$). The merit of this work lies in that not only the generation of triangular pulses with variable symmetry is performed, but also the wavelength conversion of symmetrical and asymmetrical triangular pulses has been calculated quantitatively. The demonstrated approach of generator for variable symmetry triangular waveform is promising candidate for wave-length conversion, which can be applicated in all-optical access network.

Ethics declarations

Conflicts of interest

The authors declare no conflict of interest.

References

[1] KARTHIKEYAN R, PRAKASAM S. A survey on radio over fiber (RoF) for wireless broadband access technologies[J]. International journal of computer applications, 2013, 64(12)：14-19.

[2] WANG F, DONG J, XU E, et al. All-optical UWB generation and modulation using SOA-XPM effect and DWDM-based multi-channel frequency discrimination [J]. Optics express, 2010, 18(24)：24588-24594.

[3] WANG H, LATKIN A I, BOSCOLO S, et al. Generation of triangular-shaped optical pulses in normally dispersive fiber[J]. Journal of optics, 2010, 12(3)：035205.

[4] ZHANG W, YAO J. Photonic generation of millimeter-wave signals with tunable phase shift[J]. IEEE photonics journal, 2012, 4(3)：889-894.

[5] YAO J. Photonic generation of microwave arbitrary waveforms[J]. Optics communications, 2011, 284：3723-3736.

[6] HE T, FONTAINE N K, SCOTT R P. Optical arbitrary waveform generation-based packet generation and all-optical separation for optical-label switching[J]. IEEE photonics technology letters, 2010, 22(10)：715-717.

[7] BHAMBER R S, LATKIN A I, BOSCOLO S, et al. All-optical TDM to WDM signal conversion and partial regeneration using XPM with triangular pulses[C]//2008 34th European Conference on Optical Communication, September 21-25, 2008, Brussels, Belgium. New York：IEEE, 2008：1-2.

[8] LATKIN A I, BOSCOLO S, BHAMBER R S, et al. Optical frequency conversion, pulse compression and signal copying using triangular pulses[C]//2008 34th European Conference on Optical Communication, September 21-25, 2008, Brussels, Belgium. New York：IEEE, 2008：1-2.

[9] ZHANG A, LI C. Analysis of dynamic optical arbitrary waveform generation based on three FBG arrays[J]. Optik laser technology, 2013, 52：81-86.

[10] JIANG H, YAN L, SUN Y, et al. Photonic arbitrary waveform generation based on crossed frequency to time mapping[J]. Optics express, 2013, 21(5)：6488-6496.

[11] LIU J, HUANG C, SHU C. Photonically assisted microwave waveform generation by gain-transparent SBS-induced carrier processing[J]. Optics letters, 2017, 42：3852-3855.

[12] ZHAI W, WEN A, SHAN D. Photonic generation and transmission of frequency-doubled triangular and square waveforms based on two Mach-Zehnder modulators and a Sagnac loop[J]. Lightwave technology, 2019, 37(9)：1937-1945.

[13] XIA Y, JIANG Y, ZI Y, et al. Photonic microwave waveforms generation based on pulse carving and superposition in time-domain[J]. Optics communications, 2018, 414：177-184.

[14] BAI G, HU L, JIANG Y, et al. Versatile photonic microwave waveforms generation using a dual-parallel Mach-Zehnder modulator without other dispersive elements[J]. Optics communications, 2017, 396：134-140.

[15] ZHANG F, GAO B, ZHOU P, et al. Triangular pulse generation by polarization multiplexed optoelectronic oscillator[J]. IEEE photonics technology letters, 2016, 28(15)：1645-1648.

[16] ZHANG Y, SHANG T, GAO Y, et al. A stable photonic generation scheme of triangular waveform with double frequency and variable power[J]. Modern optics, 2019, 66(12)：1318-1328.

[17] YUAN J, NING T, LI J, et al. A photonic-assisted periodic triangular-shaped pulses generator based on FWM effect in an SOA[J]. Optics communications, 2016, 381：450-456.

[18] HU J, LI J, ZHAO J, et al. A simple scheme for photonic generation of microwave waveforms using a dual-drive Mach-Zehnder modulator[J]. Applied sciences, 2020, 10(21)：7914.

[19] WANG C, NING T, LI J, et al. Photonic generation of frequency-quadrupled triangular waveform based on a DP-QPSK modulator with tunable modulation index[J]. Optics and laser technology, 2021, 137：106818.

[20] LI S, GAO X, LI H, et al. Photonic generation of frequency-doubled triangular-shaped waveforms based on a PM-MZM modulator[J]. Journal of Russian laser research, 2020, 41：521-527.

[21] LI J, WANG C, PEI L, et al. Generation of optical triangular-shaped pulse train with variable symmetry by using an I/Q modulator[J]. Optics letters, 2020, 45(6)：1411-1414.

[22] LI J, NING T, PEI L, et al. Photonic generation of triangular-shaped waveform signal with adjustable symmetrical coefficient[J]. Journal of modern optics, 2019, 66：1-9.

[23] LIU Y, LI J, HE Y, et al. Generator of signals with quadruple frequency and triangular waveform tunable in symmetry based on dual-parallel Mach-Zehnder modulator and balanced photodetector[J]. Acta optica sinica, 2021, 41(19)：1906005.

[24] PARMIGIANI F, IBSEN M, PETROPOUILOS P, et al. Efficient all-optical wavelength-conversion scheme based on a saw-tooth pulse shaper[J]. IEEE photonics technology letters, 2009, 21(24)：1837-1839.

[25] PARMIGIANI F, IBSEN M, NG T T, et al. Efficient wavelength conversion using triangular pulses generated using a superstructured fiber Bragg grating[C]//Optical Fiber Communication Conference, February 24-28, 2008, San Diego, USA. Washington, DC：Optica Publishing Group, 2008：OMP3.

[26] YUAN J, NING T, LI J, et al. Research on photonic generation of quadrupling triangular-shaped waveform using external modulation[J]. Optical fiber technology, 2018, 45：352-358.

[27] AGRAWAL G P. Nonlinear fiber optics[M]. Beijing：Publishing House of Electronics Industry, 2014：59-61.